

Physical and Optical Characterization of Manganese Ions in Sodium - Zinc - Phosphate Glass Matrix

H.A. Abd El-Ghany

Department of Engineering Mathematics and Physics, Faculty of Engineering (Shoubra),
Benha University, Cairo, 11629, Egypt.

Abstract: In order to investigate the significant modifications induced by incorporation of manganese ions in sodium-zinc-phosphate glass matrix, a glass system of chemical formula $40\text{P}_2\text{O}_5-40\text{ZnO}-(20-x)\text{Na}_2\text{O}-x\text{MnO}$ (where, x varied from 1 to 6 mol%) was prepared using the traditional melt quenching technique. The values of the glass density were increased and those of the molar volume were decreased by increasing the content of MnO. In addition, the concentration of manganese ions and the related field strength were increased while the corresponding inter-ionic spacing and polaron radius were decreased. The spectroscopic studies of all samples were carried out over (190-2500 nm) spectral range. The optical transmission of the prepared glass in the visible-near IR spectral range is enhanced by increasing the MnO content where it reaches a maximum value of about 86% at concentration 3% of MnO. This excellent transmission in such spectral range suggested the use of the present glass in many technological applications such as optical filters, IR domes, modulators, laser windows and lenses especially for Nd:YAG lasers. The optical band gap energy and the Urbach energy were determined. The refractive index was found to be decreased by increasing the MnO concentration from 1% to 3% then increased by increasing the MnO concentration from 3% to 6%. Other related physical parameters such as dielectric constant, electric susceptibility, molar polarizability and metallization criterion were evaluated. The results predicted the working of the present glass in the range of nonlinear optical materials.

Keywords: Phosphate Glass – Manganese Ions – Optical Band Gap – Refractive Index – Metallization Criterion

I. INTRODUCTION

A wide range of attractive optical, thermal, mechanical, and other physical properties make glasses the most useful class of materials in which the practicality, reliability and low cost can be combined in accordance with the specific requirements. Recently, they are used essentially in many technologically important applications including optical fibers [1], laser hosts [2], vitrification of radioactive waste [3], and biomedical engineering [4]. Phosphate glasses are particularly interesting due to several superiorities over other glass formers such as typically borate and silicate glasses. Phosphate-based glasses have evidenced high electrical conductivity, high thermal expansion coefficient, low thermal conductivity and low dispersion. Besides, they have recorded low melting and softening temperatures along with strong glass forming character [5-8]. The network structure of phosphate glasses makes them suitable hosts to incorporate a larger extent of cations in order to obtain multicomponent glass matrices [9,10]. Nevertheless, low chemical durability and volatile nature of phosphate glasses restricted their uses in many technological applications against devitrification and moisture resistant. So, intensive works have been devoted to minimize such hygroscopic nature of phosphate glasses [11].

The properties of phosphate-based glasses in terms of structural, electrical and optical properties can be greatly changed by adding a precisely amount of some oxides as network modifiers in the glass matrix. Physical properties of the modified phosphate glasses to a large extent are controlled by structural effects and nature of bonds established within the vitreous network [12-14]. Phosphate glasses modified by alkali oxides such as Na_2O are more stable due to several phosphate structural groups established during the reorganization processes causing compaction of the glass network [15]. In addition, high ionic conductivity can be predicted by such glasses [16]. Some metal oxides like Fe_2O_3 , Al_2O_3 , CaO , ZnO , etc., can be employed as good stabilizers when introduced into the P_2O_5 network leading to a noticeable increase in the chemical durability of phosphate glasses [17]. However, ZnO is well considered as a good modifier to enhance the chemical stability of phosphate glasses since Zn^{2+} ions produce appropriate structural effects which inhibit the hydration reaction [18]. Phosphate-based glasses containing transition metal ions are scientifically interesting materials due to their attractive properties which can be used in many technological applications including electronic and electro-optical devices [19,20]. Nevertheless, transition metal oxides can be dissolved easily in phosphate glasses forming several oxidation states within the glass matrix depending on the chemical composition of the glass system. On this basis, the produced glasses can acquire in many cases somewhat characteristic coloration which may be attributed to d-d electronic transitions [21].

Among various transition metal ions, manganese (^{55}Mn) is particularly attractive as it can exist in different valence states with different coordination in glass networks [22]. In borate glasses, manganese exists mainly as Mn^{3+} ions with octahedral coordination whereas in silicate and germinate glasses, it identified as Mn^{2+} ions with both tetrahedral and octahedral coordination [23]. The content of manganese in multivalent states occupying tetrahedral or octahedral sites in the glass matrix is controlled by the quantitative properties of glass formers and modifiers; ions size in the glass structure, magnitude of their field strength, mobility of the modifier cation, etc., [24]. Over the past few years, phosphate glasses containing manganese ions have been widely explored by a large number of investigations due to their structural, optical, and physical properties. The addition of manganese oxide in phosphate-based glass matrix have evidence of the formation of P—O—Mn bonds which replace the easily hydrosoluble P—O—P bonds which in turn improve the chemical durability of such glasses [25]. Mohan et al., have indicated that in phosphate-based glasses, manganese exists both as Mn^{2+} and Mn^{3+} valence states depending on the content of manganese oxide in the glass matrix [26]. At low concentration of manganese oxide, it was found that manganese ions are mostly identified as Mn^{2+} states which contribute network forming positions leading to an increase in the rigidity of the glass network. At higher concentrations of manganese oxide, these ions seem to be identified mostly as Mn^{3+} states which take the role of modifiers. Both Mn^{2+} and Mn^{3+} ions are found to exhibit paramagnetic role while Mn^{2+} ions is identified as luminescence activators. However, Mn^{2+} ions give a faint colour to the prepared glass but Mn^{3+} ions yield a deep purple colour. It must be noted that glasses melted under atmospheric conditions reveal two mixed states with the colour of the trivalent manganese is dominant [27].

In the previous study [28], the role of cadmium ions in sodium-zinc-phosphate glass matrix was investigated. The analysis indicated that the glass samples showed successive transparency in both visible and near-IR ranges of spectrum until 2500 nm with relatively high transmission. The results suggested the practicality employing such glass in manufacturing optical supplies and optical windows used for Nd:YAG lasers. The aim of the present study is to characterize the intrinsic and extrinsic modifications induced by manganese ions in the phosphate glass network. A series of manganese-sodium-zinc-phosphate glasses with the chemical composition $40\text{P}_2\text{O}_5-40\text{ZnO}-(20-x)\text{Na}_2\text{O}-x\text{MnO}$ (where, $x = 1, 2, 3, 4, 5$ and 6 mol%) have been suggested. Consequently, the influence of manganese on the physical and optical properties of the proposed glass system has to be explored.

II. EXPERIMENTAL PROCEDURE

In the present work, a glass matrix with chemical composition of $40\text{P}_2\text{O}_5-40\text{ZnO}-(20-x)\text{Na}_2\text{O}-x\text{MnO}$ (where, $x = 1, 2, 3, 4, 5$ and 6 mol%) was prepared by the conventional melt quenching method. High grade reagents of $\text{NH}_4\text{H}_2\text{PO}_4$ (ammonium dihydrogen orthophosphate), ZnO (zinc oxide), NaCO_3 (sodium carbonate) and MnO (manganese oxide) were used as starting materials. Weighing the appropriate amount of the chemicals and grinding carefully with each others in a mortar pestle for 30 minutes. The mixture is taken in a porcelain crucible and placed in a muffle furnace regulated at 260 ± 5 °C for one hour to release the residual gases such as CO_2 and NH_3 . Then the crucible was introduced to the melting furnace of 1000 ± 5 °C and let to melt for one hour. During melting, the crucible was rotated several times to obtain the maximum homogeneity of the mixture. Finally, the melt was immediately taken and casted inside the muffle furnace at 260 ± 5 °C using stainless steel mould with pressing plate by which thin disks of diameters ≈ 2.75 cm are obtained. The prepared samples were annealed at 260 ± 5 °C for one hour then the furnace is switched off and left to reach the room temperature. The annealing step is important to reduce the internal strains and cracks that might be remained within the glass during the quenching process. The density of the prepared glass samples was determined at the room temperature using the ordinary Archimedes' technique, with toluene as an immersion liquid of steady density (0.868 g/cm^3) as [29]:

$$\rho = \frac{W_{air}}{(W_{air} - W_{liq})} \rho_o \quad (1)$$

Where, W_{air} and W_{liq} are the weights of the sample in air and in liquid respectively. The molar volume was calculated using the data of molecular weight, M and density, ρ as [29]:

$$V_M = \frac{M}{\rho} \quad (2)$$

III. RESULTS AND DISCUSSIONS

3.1 XRD Examination: The prepared samples have been investigated by X-ray diffraction (XRD) technique to examine their glass formability. The diffraction data were recorded versus 2θ values between 4° and 70° as shown in Fig. 1. The results of all samples with different contents of MnO showed diffuse scattering while no sharp peaks were detected. The absence of Bragg's peaks confirms the non-crystalline nature of the prepared samples.

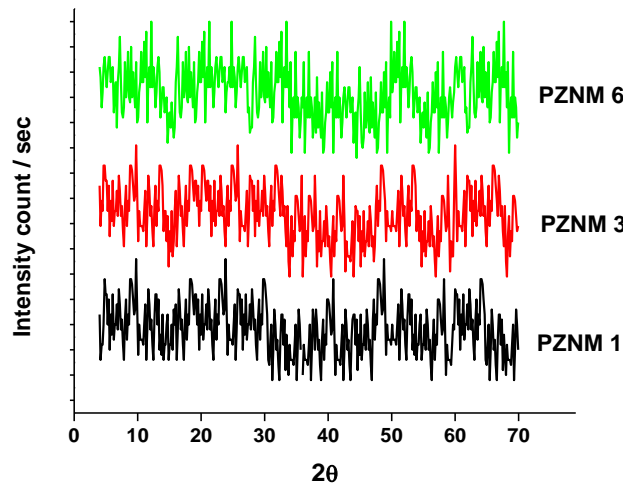


Fig. 1 XRD pattern for the glass samples.

3.2 Density and Molar Volume Measurements: The change in chemical composition in the glass matrix would have a potential effect on the density of the obtained samples. Besides, the spatial distribution of the ions within the glass network might be influenced leading to a probable change in the molar volume. Therefore, determination of the density and molar volume of the prepared glass samples is highly important in order to understand the structural changes and demonstrate the ordering of the building units in the glass network. Equations (1) and (2) were used to calculate the density, ρ and molar volume, V_M of the glass samples respectively. The experimental values of the density and the corresponding molar volume as a function of MnO concentration are listed in Table 1. The data indicate that, by increasing the content of MnO, the density is linearly increased from 2.753 gm/cm³ to 2.925 gm/cm³ while the molar volume is found to linearly decreased from 36.984 cm³ to 34.963 cm³ as depicted in Fig. 2. The increase in density seems to be qualitatively matched with that predicted by the change in chemical composition where the lower density Na₂O (2.27 gm cm⁻³) is replaced by the higher density MnO (5.43 gm cm⁻³) [30]. On the other side, the decrease in molar volume seems most likely related to the structural changes comes with the replacement of Na₂O by MnO in the glass matrix. This can be interpreted by the formation of Mn—O bonds with a covalent nature higher than that of Na—O bonds. Consequently, bond linkages of the type P—O—Mn are created as interconnections which reticulate the phosphate network and leading to close the vitreous structure [31]. Furthermore, one should expect that phosphate glass is strengthened when MnO is incorporated due to the replacement of P—O—P bonds by more P—O—Mn bonds [32].

Table 1 Experimental values of physical parameters of the prepared glass samples.

Sample Code	Density (g/cm ³)	Molar Volume (cm ³ /mole)	Ionic concentration 10 ²⁰ (ion/cm ³)	Mn-Mn Spacing (Å ^o)	Polaron radius (Å ^o)	Field strength 10 ¹⁴ (cm ²)
PZNM 1	2.753	36.984	1.629	18.312	7.378	3.674
PZNM 2	2.782	36.631	3.289	14.488	5.838	5.869
PZNM 3	2.814	36.246	4.986	12.612	5.082	7.745
PZNM 4	2.851	35.807	6.728	11.412	4.598	9.459
PZNM 5	2.887	35.392	8.509	10.554	4.252	11.062
PZNM 6	2.925	34.963	10.336	9.890	3.985	12.593

The ionic concentration of manganese and other related significant parameters can be calculated using the following relations [33]:

$$\text{Ionic concentration, } N(\text{ions/cm}^{-3}) = \frac{(\text{Avogadr o's No.}) (\text{mole \% of cation}) (\text{glass density})}{(\text{glass average molecular weight})} \quad (3)$$

$$\text{Mean spacing between manganese ions, } r_i(\text{Å}^o) = (1/N)^{\frac{1}{3}} \quad (4)$$

$$\text{Polaron radius, } r_p(\text{Å}^o) = \frac{1}{2}(\pi/6N)^{\frac{1}{3}} \quad (5)$$

$$\text{Field strength, } F(\text{cm}^2) = Z/r_p^2 \quad (6)$$

Where, Z is the valence of manganese ions. The calculated values of ionic concentration, mean spacing between manganese ions, polaron radius and field strength as a function of MnO content are listed in Table 1. The calculated values of mean Mn—Mn spacing and polaron radius are found to be decreased by increasing MnO concentration. This is most likely related to a decrease in the activation energy when MnO is incorporated [34]. It can be clearly indicated that the calculated values of the polaron radius are smaller than that of the mean Mn—Mn spacing for all batches as depicted in Fig. 3. However, the decrease in the polaron radius indicates an increase in the polarizability of a material. It can be indicated that both ionic concentration and field strength are increased by increasing MnO concentration which seem to be related to the decrease in Mn—Mn spacing. By increasing content of MnO, higher values of field strength around the manganese ions are generated which might be responsible for the shortening of phosphate chain length leading to stabilizing the glass structure [32].

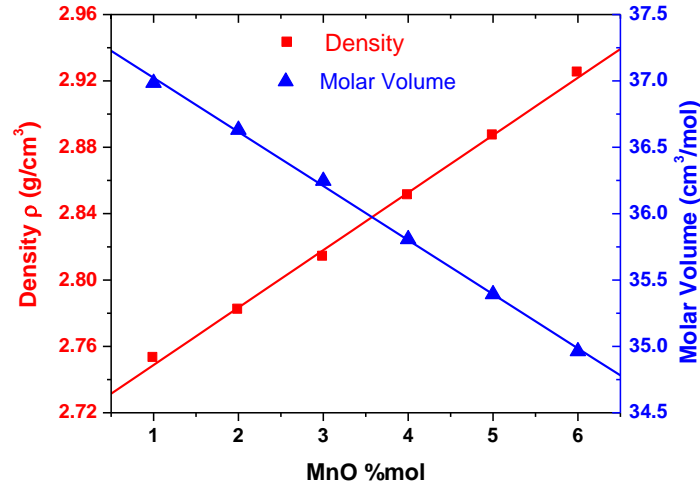


Fig. 2 Density and molar volume as a function of MnO content.

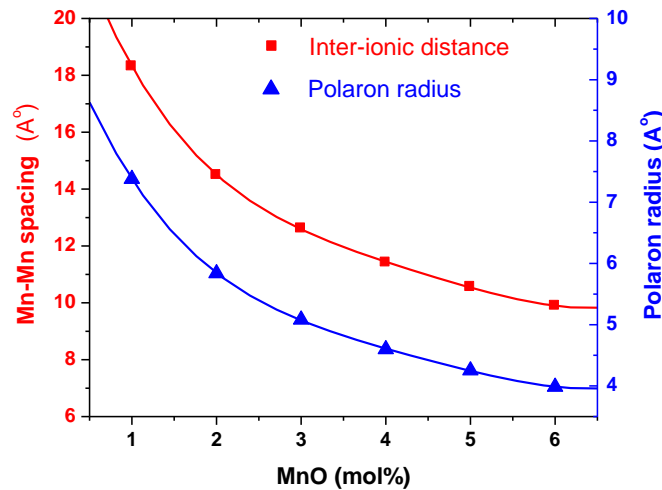


Fig. 3 Variation of manganese ions separation and polaron radius for different MnO contents.

3.3 Optical Absorption/Transmission Studies: The optical spectroscopic studies have been achieved over UV-visible-near IR spectral range in the wavelength interval of (190 – 2500 nm). The optical absorption of the glass samples is very helpful to study the electronic transitions and figure out the band structure in amorphous materials. However, the absorption spectra of the prepared samples can be used to calculate the corresponding absorption coefficient as a function of the photon wavelength according to relation [35]:

$$\alpha(\lambda) = 2.303 (A/t) \tag{7}$$

Where, A is the absorbance and t is the thickness of the glass sample. Fig. 4 shows the wavelength dependence of the absorption coefficient near and below the fundamental absorption edge for different contents of MnO. It is quite clear

that there are no sharp absorption edges which confirm the amorphous nature of the prepared glass samples [36]. It can be observed that the absorption due to the glass samples is decreased by increasing the concentration of MnO from 1% to 3% then the absorption is increased for higher concentrations of MnO till 6%. Nevertheless, the absorption edge is found to be shifted towards lower wavelength by increasing the concentration of MnO from 1% to 3% then it exhibit a red shift at higher concentrations of MnO till 6%. This seems to be related to the change in glass composition which suggested that manganese ions play a dual role when MnO is incorporated in the glass matrix. Such duality can be explained throughout the determination of the optical band gap energy since it provides a picture of the band structure within the prepared glass samples.

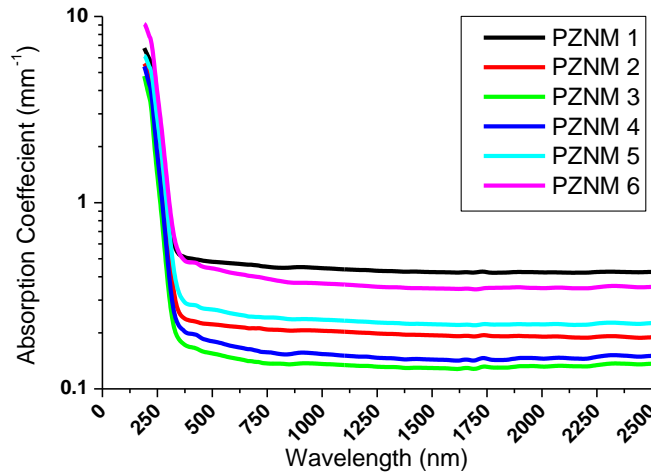


Fig. 4 Absorption coefficient of the prepared glass as a function of MnO content..

According to the relations proposed by Mott and Davies, the optical band gap energy, E_g can be determined in the high-absorption region as [37,38]:

$$\alpha h\nu = B (h\nu - E_g)^n \tag{8}$$

Where, B is constant and n is an index associated to the mechanism of inter-band electronic transitions. In the above equation the value of $n = 1/2, 2, 3/2$ or 3 according to direct allowed transitions, indirect allowed transitions, direct forbidden transitions or indirect forbidden transitions respectively. It is convenient to take $n = 2$ when dealing with glassy state referring to indirect absorption mechanism in which the interactions with lattice vibrations is involved [28]. Therefore, the optical band gap can be evaluated by plotting of $(\alpha h\nu)^{1/2}$ versus $h\nu$ as shown in Fig. 5. The plots are observed to be linear near the fundamental absorption edge in the region of strong absorption hence, the optical band gap can be determined by extrapolating the linear portion of the graph to $(\alpha h\nu)^{1/2} = 0$. The experimental values of the optical band gap are listed in Table 2.

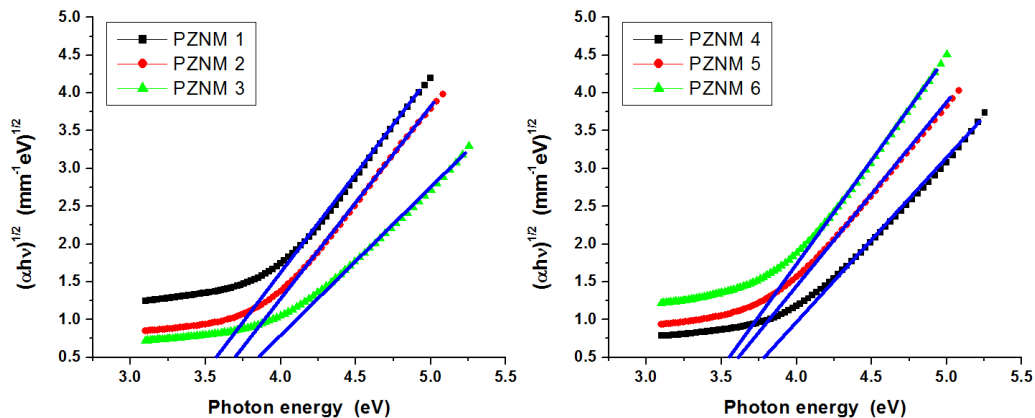


Fig. 5 Determination of the optical band gap energy.

Nevertheless, the glass system is exposed to a remarkable degree of disorder caused by the absorption of photons having energies less than that of the band gap due to existence of some localized states inside the energy gap [5]. Such

localized states constitute what is so called band tails within the energy gap that can be estimated by Urbach energy, ΔE using the Urbach rule [37]:

$$\alpha = \alpha_0 \exp(-hv/\Delta E) \tag{9}$$

Where, α is the absorption coefficient, α_0 is constant. As shown in Fig. 6, ΔE can be easily determined from the logarithmic plots of the absorption coefficient versus $h\nu$ and taking the reciprocal value of the slope associated the linear region. The experimental values of the Urbach energy are listed in Table 2. The Urbach energy and optical gap energy have opposite trends as shown in Fig. 7. By increasing the MnO concentration from 1% to 3%, the Urbach energy is decreased from 0.551 eV to 0.477 eV and the optical gap energy is increased from 3.57 eV to 3.86 eV. For higher MnO concentrations after 3% to 6%, the Urbach energy is increased from 0.477 eV to 0.563 eV and the optical gap energy is decreased from 3.86 eV to 3.54 eV. This can be explained on the basis that when a substance works as an intermediate (i.e., take a character of network former); the optical band gap is increased and when the substance acts as a modifier; the optical band gap is decreased [39]. However, manganese ions can occur in several valence states with several coordinations in the glass network. They exist both as Mn^{2+} and Mn^{3+} valence states depending on the content of manganese oxide in the glass matrix as mentioned by an earlier work of Mohan et al., 2008 [26]. At low concentration of manganese oxide, manganese ions are mostly identified as Mn^{2+} states which contribute network forming positions and their increase on the expense of Na^{2+} modifier ions causes a decrease the localized states within the energy gap as determined by ΔE . Hence, the optical gap energy is found to be increased. At higher concentrations of manganese oxide, manganese ions seem to be identified mostly as Mn^{3+} states which work as network modifiers causing some structural changes leading to an increase of the localized states within the energy gap as observed by ΔE . Hence, the optical gap energy is found to be decreased. This is agreed with the observed behavior of the absorption edge previously mentioned.

Table 2 Optical gap energy, fundamental absorption edge and Urbach energy for the glass samples.

Sample Code	Optical Gap Energy (eV)	Fundamental Absorption Edge (nm)	Urbach Energy (eV)
PZNM 1	3.57	347	0.551
PZNM 2	3.69	335	0.495
PZNM 3	3.86	321	0.477
PZNM 4	3.76	329	0.512
PZNM 5	3.61	343	0.541
PZNM 6	3.54	350	0.563

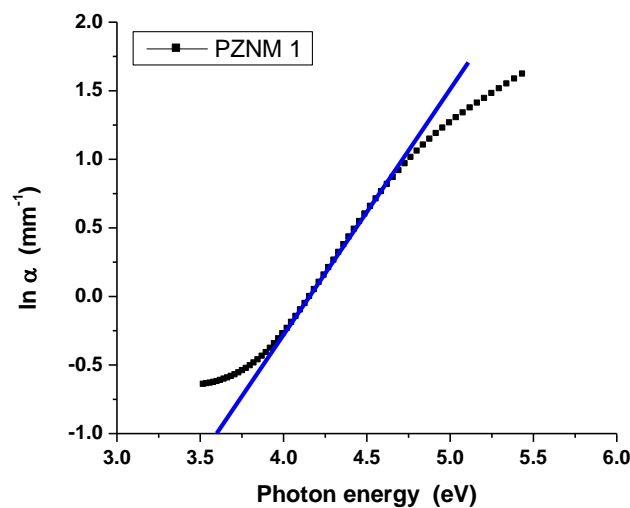


Fig. 6 A representative example for determination of Urbach energy.

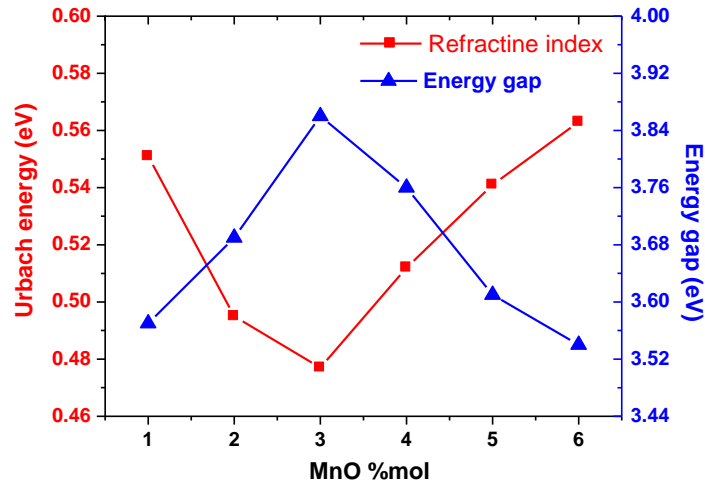


Fig. 7 Optical gap energy and Urbach energy as a function of MnO content.

On the other hand, the optical transmission of the prepared glass samples has been recorded over UV-visible-near IR spectral range in the wavelength interval of (190 – 2500 nm). Fig. 8 shows the wavelength dependence of the transmittance of the prepared glass samples for different contents of MnO. A general increase in the transmittance is observed by increasing the concentration of MnO from 1% to 3% then the transmittance is decreased for higher concentrations of MnO till 6%. This can be explained in view of the structural changes in the glass network where the optical transmission of the glass is oppositely related to the absorption behavior. Comparing the present data with that of the previous work [28], it can be observed that the transparency of the prepared glass in the visible-near IR spectral range is improved where it reaches a maximum value of about 86% at concentration 3% of MnO. With such higher transmission, the present glass is suggested to join the family of new glasses which can be used effectively in different optical applications such as optical filters, IR domes, modulators, lenses and laser windows especially for Nd:YAG lasers because their fundamental and second harmonic modules of typically emit light in IR-range of 1064 nm and visible range of 532 nm respectively.

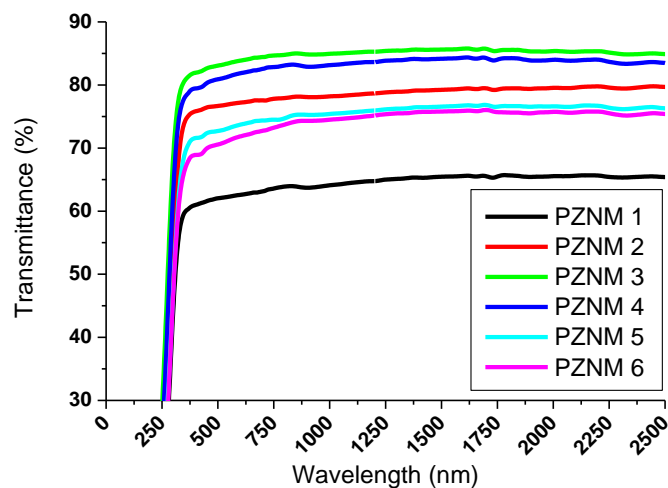


Fig. 8 Transmission spectra for the glass samples with different CdO content.

3.4. Refractive Index: The refractive index is an important physical parameter when dealing with glass systems due to its significant effect on the interaction of light with the material constituents. The refractive index, n is related to the optical gap energy through Lorenz–Lorenz equation as [40,41]:

$$\frac{n^2-1}{n^2+2} = 1 - \frac{\sqrt{E_g}}{20} \tag{10}$$

Where, E_g is the band gap energy. The calculated values of the refractive index for different contents of MnO are listed in Table 3. The data reveal a decreasing trend followed by an increase in the refractive index by increasing MnO concentration as shown in Fig. 9. This can be explained in view of the structural modifications produced due to the compositional change in chemical formula of the glass when MnO is incorporated. It turns out that the refractive index is decreased by increasing the MnO concentration from 1% to 3% where manganese acts as intermediate (i.e., share as network formers) then the refractive index is increased by increasing the MnO concentration from 3% to 6% where manganese takes up the role of a modifier. Nevertheless, the change in refractive index causes changing of the velocity of light passing through the materials influencing their overall transmittance. Hence, the optical transmission the glass can be expected in the view of refractive index evaluation [42]. In other words the lower the value of refractive index, the higher the optical transmittance of the glass; and this agrees well with the results indicated by the transmission spectra of the present glass samples.

Table 3 Refractive index, Dielectric constant, electric susceptibility, molar polarizability and Metallization criteria for different MnO concentrations.

Sample Code	Refractive index	Dielectric constant	R_M/V_M	Electric susceptibility	Molar polarizability (\AA^3)	Metallization criteria
PZNM 1	2.26	5.10	0.578	0.326	8.472	0.422
PZNM 2	2.23	4.98	0.570	0.317	8.288	0.430
PZNM 3	2.20	4.83	0.561	0.305	8.061	0.439
PZNM 4	2.22	4.92	0.566	0.312	8.044	0.434
PZNM 5	2.25	5.06	0.575	0.323	8.074	0.425
PZNM 6	2.27	5.13	0.579	0.329	8.033	0.421

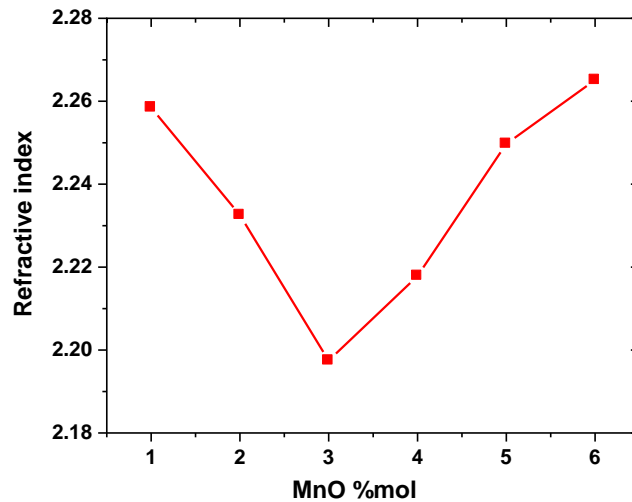


Fig. 9 The compositional dependence of refractive index of the prepared glass.

3.4. Dielectric Constant, Electric Susceptibility and Polarizability

The dielectric constant can be calculated from the refractive index using the relation [43]:

$$\epsilon = n^2 \tag{11}$$

The electric susceptibility measures the degree of polarization of a material when exposed to an external electrical field and can be given as [44]:

$$\chi = \frac{(n^2-1)}{4\pi} \tag{12}$$

The molar refraction measures of the total polarizability of one mole of a material and can be calculated in terms of refractive index and molar volume as [45]:

$$R_M = \frac{n^2-1}{n^2+2} V_M \tag{13}$$

Using Lorenz–Lorenz formula, the molar polarizability of the material can be evaluated as [45]:

$$\alpha_M = \frac{3}{4\pi N_A} R_M \tag{14}$$

Where, N_A is the Avogadro’s number. The calculated values of the dielectric constant, electric susceptibility and molar polarizability are listed in Table 3. The evaluated values are found to be mainly influenced by the change in the chemical composition of the glass. This seems to be related to structural modifications due to the replacement of Na_2O by MnO .

3.4. Metallization Criterion: Metallization criterion is an important parameter to investigate the non-metallic nature of materials hence it can be employed in order to examine the insulating behavior of the prepared glass. Herzfeld theory of metallization in the condensed matter implies that if $R_M/V_M \geq 1$ then the material is expected to have a metallic nature and if $R_M/V_M \leq 1$ then the material have to be non-metallic in nature [46]. It is clear that the present glass samples have a non-metallic nature as indicated in Table 3. Moreover, the decrease in R_M/V_M value implies that the width of both valence and conduction bands becomes small leading to large band gap and vice versa. The metallization criteria in terms of the molar refraction and molar volume can be calculated as [47]:

$$M = 1 - (R_M/V_M) \tag{15}$$

The experimental values of metallization criterion are listed in Table 3 and depicted in Fig. 10. Dimitrov and Sakka [48] have reported that materials with metallization criterion of approximately 0.30–0.45 are promising due to their nonlinear optical behavior. The present glass samples showed a metallization criterion of approximately 0.421–0.439 which introduces them as a new member in the family of nonlinear optical materials.

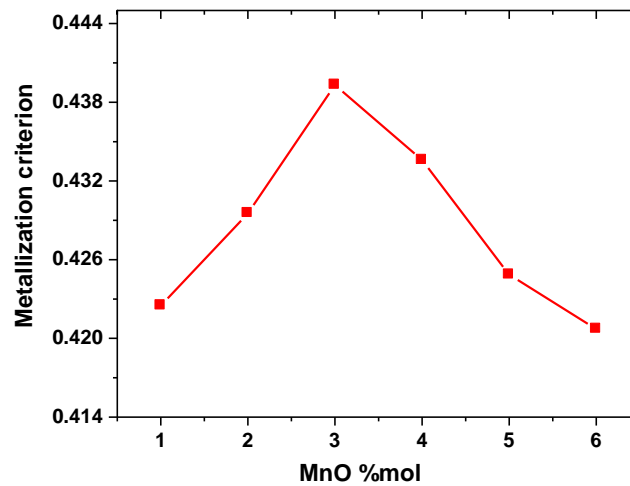


Fig. 10 Metallization criterion of the prepared glass.

CONCLUSION

A glass system of chemical formula $40P_2O_5-40ZnO-(20-x)Na_2O-xMnO$ (where, x varied from 1 to 6 mol%) has been prepared using the conventional melt quenching technique. The amorphous nature of the prepared glass is examined by the XRD technique. The values of the density are increased from 2.753 gm/cm^3 to 2.925 gm/cm^3 and those of the molar volume are decreased from 36.984 cm^3 to 34.963 cm^3 by increasing the content of MnO . The calculated values of the polaron radius are smaller than that of the mean $Mn-Mn$ spacing for all batches. The decrease in the polaron radius implies an increase in the polarizability of a material when MnO is incorporated. Furthermore, the field strength around the manganese ions is increased leading to shortening of phosphate chain length which stabilizes the glass structure. The absorption studies indicate shifting of the absorption edge towards lower wavelength by increasing the concentration of MnO from 1% to 3% then it exhibit a red shift at higher concentrations of MnO till 6%. The optical transmission of the prepared glass in the visible-near IR spectral range is enhanced by increasing the MnO content where it reaches a maximum value of about 86% at concentration 3% of MnO . This excellent transmission in such spectral range suggested the use of the present glass in many technological applications such as optical filters, IR domes, modulators, laser windows and lenses especially for $Nd:YAG$ lasers. The optical band gap is found to be ranged between 3.56 eV and 3.54 eV. The refractive index is decreased by increasing the MnO concentration from 1% to 3% then increased by increasing the MnO concentration from 3% to 6%. The data of metallization criterion reveals non-

metallic nature of the prepared samples. Moreover, the results predicted the working of the present glass in the range of nonlinear optical materials.

ACKNOWLEDGMENT

Deep thanks to **Dr. Ahmed El-Basaty**, Faculty of Industrial Education, Helwan University; for his help and facilitating the use the equipment for preparing the glass samples.

REFERENCES

- [1]. M. Yamane, Y. Asahara, "Glasses for Photonics", Cambridge University Press (2005).
- [2]. J.H. Campbell, J.S. Hayden and A. Marker, "High-power solid-state lasers: a laser glass perspective", *Int. J. Appl. Glass Sci.*, vol. 2, pp. 3-29, 2011.
- [3]. P. Bergo, S.T. Reis, W.M. Pontuschka, J.M. Prison and C.C. Motta, "Dielectric properties and structural features of barium-iron phosphate glasses" *J. Non-Cryst Solids*, vol. 336, pp. 159-164, 2004.
- [4]. A.G. Dias, J.M. Skakle, I.R. Gibson, M.A. Lopes and J.D. Santos, "In situ thermal and structural characterization of bioactive calcium phosphate glass ceramics containing TiO₂ and MgO oxides: high temperature-XRD studies", *J. Non-Cryst Solids*, vol. 351, pp. 810-817, 2005.
- [5]. H. Abd El-Ghany, "Cadmium Doped Copper Containing Phosphate Glass as a Bandpass Filter for Solar Cell Protection", *J. Adv. Phys.*, vol. 14, pp. 5488-5503, 2018.
- [6]. M.A. Karakassides, A. Saranti, I. Koutselas, "Preparation and structural study of binary phosphate glasses with high calcium and/or magnesium content", *J. Non-Cryst Solids*, vol. 347, pp. 69-79, 2004.
- [7]. S.T. Reis, M. Karabulut, D.E. Day, "Chemical durability and structure of zinc-iron phosphate glasses", *J. Non-Cryst. Solids*, vol. 292, pp. 150-157, 2001.
- [8]. R.K. Brow, "Review: the structure of simple phosphate glasses", *J. Non-Cryst. Solids*, vol. 263-264, pp.1-28, 2000.
- [9]. B.P. Choudhary, S. Rai and N.B. Singh, "Properties of silver phosphate glass doped with nanosize zinc oxide", *Ceram. Int.*, vol. 42, pp. 10813-10825, 2016.
- [10]. H.A. Abd El-Ghany, "Characterization and Optical Properties of MnO Doped CuO-Containing Phosphate Glass as Absorption Filters", *J. Adv. Phys.*, vol. 15, pp. 5983-5996, 2018.
- [11]. S. Li, Y. Lu, Y. Qu, Y. Xu, L. Ming, Z. Song and Y. Yue, "Influences of ZnO on the chemical durability and thermal stability of calcium iron phosphate glasses", *J. Non-Cryst. Solids*, vol. 498, pp. 228-235, 2018.
- [12]. Y. Li, J. Yang, S. Xu, G. Wang and L. Hu, "Physical and Thermal Properties of P₂O₅-Al₂O₃-BaO-La₂O₃ Glasses", *J. Matter. Sci. Technol.*, vol. 21, pp. 391-394, 2005.
- [13]. M. Ahmad, F. Salman, M. Morsi, K. El-Badry and F. Metwall, "Electrical Properties of Some Copper-Containing Phosphate Glasses", *J. Mater. Sci.*, vol. 41, pp. 1667-1669, 2006.
- [14]. X. Li, H. Yang, X. Song and Y. Wu, "Glass forming region, structure and properties of zinc iron phosphate glasses", *J. Non Cryst. Solids*, vol. 379, pp. 208-213, 2013.
- [15]. Y.M. Moustofa, K. El-Egili, "Infrared spectra of sodium phosphate glasses", *J. Non-Cryst. Solids*, vol. 240, pp. 144-153, 1998.
- [16]. A. Magistris, "Ionic Conduction in Glasses" In: B. Scrosati, A. Magistris, C.M. Mari and G. Mariotto, "Fast Ion Transport in Solids", NATO ASI Series (Series E: Applied Sciences), Springer, vol 250, pp. 213-230, 1993.
- [17]. G. Sahaya Baskaran, G. Little Flower, D. Krishna Rao and N. Veeraiah, "Structural role of In₂O₃ in PbO-P₂O₅-As₂O₃ glass system by means of spectroscopic and dielectric studies, *J. Alloy. Compd.*, vol. 431, pp. 303-312, 2007.
- [18]. K. Suzuya, K. Itoh, A. Kajinami and C.K. Loong, "The structure of binary zinc phosphate glasses", *J. Non-Cryst. Solids*, vol. 345-346, pp. 80-87, 2004.
- [19]. Y. Sakurai and J. Yamaki, "V₂O₅-P₂O₅ Glasses as Cathode for Lithium Secondary Battery", *J. Electrochem. Soc.*, vol. 32, pp. 512-513, 1985.
- [20]. A. Margaryan, J.H. Choi and F.G. Shi, "Spectroscopic properties of Mn²⁺ in new bismuth and lead contained fluorophosphate glasses", *Appl. Phys. B*, vol. 78, pp. 409-413, 2004.
- [21]. N. Zotov, H. Schlenz, B. Brendebach, H. Modrow, J. Hormes, F. Reinauer, R. Glaumc, A. Kirfel, and C. Paulmann, "Effects of MnO-Doping on the Structure of Sodium Metaphosphate Glasses", *Z. Naturforsch.*, vol. 58a, pp. 419-428, 2003.
- [22]. I. Bratu, I. Ardelean, A. Barbu, V. Mih, D. Maniu and G. Botezan, "Spectroscopic investigation of some lead phosphate oxide glasses containing manganese ions", *J. Mol. Struct.*, vol. 482-483, pp. 689-692, 1999.
- [23]. A. Van Die, A.C.H.I. Leenaers, G. Blasse and W.F. Van Der Weg, "Germanate glasses as hosts for luminescence of Mn²⁺ and Cr³⁺", *J. Non-Cryst. Solids*, vol. 99, pp. 32-44, 1988.
- [24]. S. Sreehari Sastry and B. Rupa Venkateswara Rao, "Spectroscopic characterization of manganese-doped alkaline earth lead zinc phosphate glasses", *Bull. Mater. Sci.*, Vol. 38, pp. 475-482, 2015.
- [25]. P. Pascuta, G. Borodi, N. Jumate, I. Vida-Simiti, D. Viorel and E. Culea, "The structural role of manganese ions in some zinc phosphate glasses and glass ceramics" *J. Alloy. Compd.*, vol. 504, pp. 479-483, 2010.
- [26]. N. Krishna Mohan, M. Rami Reddy, C.K. Jayasankar and N. Veeraiah, "Spectroscopic and dielectric studies on MnO doped PbO-Nb₂O₅-P₂O₅ glass system", *J. Alloy. Compd.*, vol. 458, pp. 66-76, 2008.
- [27]. M. Tomozawa and Robert H. Doremus, "Treatise on Materials Science and Technology, Volume 12: Glass I: Interaction with Electromagnetic Radiation, Elsevier, 2017.
- [28]. H.A. Abd El-Ghany, "Development of a New Glass for Both Visible and Near-Infrared Optical Applications", *Key Eng. Mater.*, vol. 786, pp. 224-235, 2018.
- [29]. Y.H. Elbashaar, H.A. Abd El-Ghany, "Optical spectroscopic analysis of Fe₂O₃ doped CuO containing phosphate glass", *Opt. Quant. Electron.* 49:310, pp. 1-13, 2017.
- [30]. A.M. Nassar, M.M. El Oker, Sh. N. Radwan and E. Nabhan, "Effect of MO (CuO, ZnO, and CdO) on the compaction of sodium meta phosphate sealing glass", *Curr. Sci. Int.*, vol. 2, pp. 1-7, 2013.
- [31]. W. Ahmina, M. El Moudane, M. Zriouil and M. Taibi, "Glass-forming region, structure and some properties of potassium manganese phosphate glasses", *Phase Transit.*, vol. 89, pp. 1-11, 2016
- [32]. R.O. Omrani, S. Krimi, J.J. Videau, I. Khattech, A. El Jazouli and M. Jemal, "Structural investigations and calorimetric dissolution of manganese phosphate glasses", *J. Non-Cryst. Solids*, vol. 389, pp. 66-71, 2014.
- [33]. A.S. Rao, Y.N. Ahammed, R.R. Reddy, T.V.R. Rao, "Spectroscopic studies of Nd³⁺-doped alkali fluoroborophosphate glasses", *Opt. Mater.*, vol. 10, pp. 245-252, 1998.

- [34]. M.M. Ahmed, C.A. Hogarth and M.N. Khan, "A study of the electrical and optical properties of the GeO₂-TeO₂ glass system", *J. Mater. Sci. Lett.*, vol. 19, pp. 4040-4044, 1984.
- [35]. S.K.J. Al-Ani, I.H.O. Al-Hassany and Z.T. Al-Dahan, "The optical properties and a.c. conductivity of magnesium phosphate glasses", *J. Mater. Sci.*, vol. 30, pp. 3720-3729, 1995.
- [36]. S.A. Siddiqi, M. Masih, A. Mateen, "Optical band gap in Cd-Mn-phosphate glasses Materials", *Mater. Chem. Phys.*, vol. 40, pp. 69-72, 1995.
- [37]. M. Altaf and M. A. Chaudhry, "Effect of MnO on the Optical Band Gap in MnO-CdO-P₂O₅ Glasses", *J. Korean Phys. Soc.*, vol. 36, pp. 265-268, 2000.
- [38]. S.F. Khor, Z.A. Talib, F. Malek and E.M. Cheng, "Optical properties of ultraphosphate glasses containing mixed divalent zinc and magnesium ions" *Opt. Mater.*, vol. 35, pp. 629-633, 2013.
- [39]. M. A. Chaudhry, M. Altaf, "Optical absorption studies of sodium cadmium phosphate glasses", *Mater. Lett.*, vol. 34, pp. 213-216, 1998.
- [40]. B. Eraiah, Sudha G. Bhat, "Optical properties of samarium doped zinc-phosphate glasses", *J. Phys. Chem. Solids*, vol. 68, pp. 581-585, 2007.
- [41]. Y. Wang, S. Dai, F. Chen, T. Xu and Q. Nie, "Physical properties and optical band gap of new tellurite glasses within the TeO₂-Nb₂O₅-Bi₂O₃ system", *Mater. Chem. Phys.*, vol. 113, pp. 407-411, 2009.
- [42]. Ch. Tirupataiah, T. Narendrudu, S. Suresh, P. Srinivasa Rao, P.M. Vinaya Teja, M.V. Sambasiva Rao, G. Chinna Ram and D. Krishna Rao, "Influence of valence state of copper ions on structural and spectroscopic properties of multi-component PbO-Al₂O₃-TeO₂-GeO₂-SiO₂ glass ceramic system- a possible material for memory switching devices", *Opt. Mater.*, vol. 73, pp. 7-15, 2017.
- [43]. B. Bendow, P. Benerjee, M. Drexhage, J. Lucas, "Polarized Raman scattering in rare-earth fluoride glasses". *J. Am. Ceram. Soc.*, vol. 65, pp. C92-C95, 1985.
- [44]. S.A. Umara, M.K. Halimah, K.T. Chan, A.A. Latif, "Polarizability, optical basicity and electric susceptibility of Er³⁺ doped silicate borotellurite glasses", *J. Non-Cryst. Solids*, vol. 471, pp. 101-109, 2017.
- [45]. Y.J. Cha, J.H. Kim, J.-H. Yoon, B.S. Lee, S. Choi, K.S. Hong, E.D. Jeong, T. Komatsu, H.G. Kim, "Synthesis, electronic polarizability and β-BaB₂O₄ crystallization in BaO-B₂O₃-TeO₂ glasses, *J. Non-Cryst. Solids*, vol. 429, pp. 143-147, 2015.
- [46]. M. Halimah, M. Fazmy, M. Azlan, H. Sidek, "Optical basicity and electronic polarizability of zinc borotellurite glass doped La³⁺ ions", *Results Phys.*, vol. 7, pp. 581-589, 2017.
- [47]. N. Berwal, S. Dhankhar, P. Sharma, R.S. Kundu, R. Punia, N. Kishore, Physical, structural and optical characterization of silicate modified bismuth-borate-tellurite glasses, *J. Mol. Struct.* 1127 (2017) 636-644.
- [48]. V. Dimitrov and S. Sakka, "Linear and nonlinear optical properties of simple oxides. II", *J. Appl. Phys.*, vol. 79, pp. 1741-1745, 1996.